

# Empirical path-loss model in train car

Sam Aerts, David Plets, Leen Verloock, Emmeric Tanghe, Wout Joseph, and Luc Martens

Department of Information Technology

Ghent University / iMinds

B-9050 Ghent, Belgium

Email: sam.aerts@intec.ugent.be

**Abstract**—In this study, path loss measurements were performed in a train environment at five frequencies used in present and future wireless communication technologies, considering various transmitter (Tx) - receiver (Rx) configurations. First, a one-slope path-loss model was constructed for each frequency. Path loss exponents below 1.5 at lower frequencies ( $\sim 1$  GHz) indicate a waveguide effect, while the influence of the seats on the propagation at higher frequencies ( $\sim 2$  GHz) results in exponents larger than 2. Finally, a single, frequency-dependent path-loss model was fitted to the total data pool, resulting in a model with a coefficient of determination,  $R^2$ , of 0.77.

**Index Terms**—propagation; path loss; frequency-dependent model; train

## I. INTRODUCTION

In a society increasingly dependent on wireless communication, the railway environment is slowly lagging behind. A steady data or voice connection in trains is often a problem, due to the large car-body penetration loss, the frequent handovers, and the scarcity of track-side base stations in rural areas. A possible solution to this problem would be the deployment of a miniature WiFi-like base station (e.g., a femtocell) in a train car, to which users can connect directly instead of to a macrocell base station.

However, studies on propagation characteristics in train environments are scarce in literature. There have been some simulation studies [1], and studies on train-to-wayside communication [2], but to our knowledge, there has only been a single study on path loss measurements in train cars [3], which considered a frequency of 2200 MHz for intra-car communication.

The goal of this study is to construct a frequency-dependent model of the path loss in a train environment. To this end, path loss measurements are performed in a non-moving double-decker train car at five different frequencies used in present and future wireless communications, namely 900 MHz (Global System for Mobile Communications technology, or GSM900), 1800 MHz (GSM1800), 2100 MHz (Universal Mobile Telecommunications System technology, or UMTS), and 800 and 2600 MHz (Long Term Evolution technology, or LTE), and are fitted to individual one-slope models for each frequency to assess whether a trend can be observed. Finally, the total data pool is then fitted to a single, frequency-dependent, path-loss model.



Fig. 1. Receiver setup, with a receiver antenna (Rx) mounted on a trolley, and connected to a spectrum analyzer and a tachometer.

## II. MATERIALS AND METHODS

All measurements are performed in a non-moving double-decker train car, of type M6, built by Bombardier (Montréal, Canada) and Alstom (Levallois-Perret, France), and put at our disposal by the NMBS (Nationale Maatschappij der Belgische Spoorwegen).

The measurement setup includes a transmitter as well as a receiver part. The transmitted part consists of a transmitter antenna (Tx) connected to a Rohde & Schwarz SMP22 signal generator. The receiver part (shown in Figure 1) consists of a receiver antenna (Rx) connected to a Rohde & Schwarz FSL6 spectrum analyzer, and a tachometer, which is used to measure the covered distance. As Tx and Rx, identical, vertically polarized omnidirectional antennas are used, of the brand European Antennas, model XPO2V-0.3-10.0/1381.

The Tx is positioned just below the ceiling, at a height of

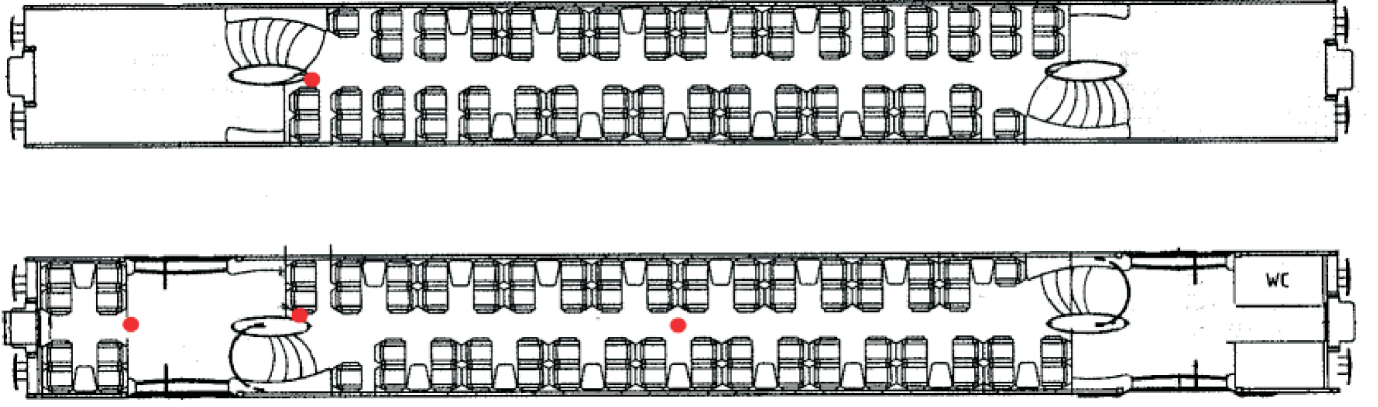


Fig. 2. On this schematic of the train car's upper (above) and lower (below) floors, the transmitter (Tx) locations are indicated by red dots. In total, the Tx was mounted at four positions; two downstairs (at the front, and in the middle), one in the entrance-hallway (on the far left on the schematic), and one upstairs (at the front).

about 1.8 m above the floor, at locations deemed to represent suitable locations for wireless stations (shown on Figure 2); the Tx is placed twice on the first floor (at the front and in the middle), once on the second floor (at the front), and once in the entrance-hallway, which has stairs (and plexiglass doors) going to the two floors. The Rx, in its turn, is mounted on a trolley, at a height of approximately 1.3 m above the floor, and is moved on a path along the corridor (the corridor on the same floor as the Tx, or on both floors when the Tx is positioned in the entrance-hallway). While moving, samples of the received power and the travelled distance are collected. In order to estimate the local mean power, the Rx paths are subdivided in intervals of length 10 wavelengths, with the average of the measured power levels over these intervals, denoted as  $P_R$ , associated with the centre of the interval [4].

In addition to the corridor measurements described above, path loss measurements are also performed at 33 of the 66 available seats on the first floor (as seen on the lower schematic in Figure 2), with the Rx being held in front of the experimenter sitting on a seat, at a height of approximately 1.3 m above the floor, and the Tx positioned at the front of the corridor, just below the ceiling. During each of these measurements, 200 samples of the received power are collected, of which the average received power,  $P_R$ , is calculated.

Following the received-power measurements, the path-loss values,  $PL$  (in dB), are calculated using the following link budget:

$$PL = P_T + G_T + G_R - L_T - L_R - P_R, \quad (1)$$

with  $P_T$  (in dBm) the transmitter power (here, approximately 25 dBm),  $G_T$  and  $G_R$  (in dBi) the Tx and Rx antenna gains,  $L_T$  and  $L_R$  (in dB) the antenna cable losses.

For each frequency, the results of the various Tx-Rx configurations are then combined and used to construct a one-slope path-loss model [5], [6], which expresses the path loss (in dB) as a function of the distance  $d$  (in m) between the Tx and the Rx:

$$PL(d) = PL(d_0) + 10n \cdot \log_{10}(d/d_0) + \chi_S, \quad (2)$$

TABLE I  
PARAMETERS OF THE FITTED ONE-SLOPE MODELS ( $d_0 = 1$  m) FOR EACH FREQUENCY

$f$ [MHz]	$PL(d_0)$ (CI) [dB]	$n$ (CI) [-]	$\sigma_S$ [dB]	$R^2$ [-]
800	32.96 (27.74, 38.18)	1.39 (0.82, 1.97)	5.56	0.32
900	33.97 (29.36, 38.57)	1.47 (0.95, 1.98)	4.89	0.40
1800	37.86 (34.44, 41.28)	2.09 (1.72, 2.47)	4.24	0.62
2100	40.74 (37.66, 43.82)	1.94 (1.61, 2.28)	4.03	0.61
2600	41.62 (38.98, 44.35)	2.33 (2.04, 2.63)	3.94	0.71

with  $PL(d_0)$  (in dB) the path loss at an arbitrarily chosen reference distance  $d_0$  (in m) (here,  $d_0 = 1$  m),  $n$  the dimensionless path loss exponent, and  $\chi_S$  a lognormally distributed variable, with median 0 dB and variance  $\sigma_S^2$ , representing shadow fading.

Finally, the total pool of path-loss results is fitted to a frequency ( $f$ , in GHz) and distance ( $d$ , in m) dependent path-loss model, based on the one-slope and Walfish-Ikegami models [5]:

$$PL(d, f) = PL(d_0, f_0) + 20 \log_{10}\left(\frac{f}{f_0}\right) + 10n(f) \log_{10}\left(\frac{d}{d_0}\right) + \epsilon_S, \quad (3)$$

with  $PL(d_0, f_0)$  (in dB) the path loss at arbitrarily chosen reference distance,  $d_0$  (here, 1 m), and frequency,  $f_0$  (here, 1 GHz), and  $n(f)$  the dimensionless path loss exponent, with assumed linear dependency on the frequency, of the form

$$n(f) = n_0 + m \cdot f, \quad (4)$$

with  $n_0$  (dimensionless) and  $m$  (in  $\text{GHz}^{-1}$ ) two parameters to be fitted.  $\epsilon_S$  is, analogous to the one-slope model of Equation (2), a lognormally distributed variable, with median 0 dB and variance  $\rho_S^2$ , representing shadow fading. It should be noted that, as in the Walfish-Ikegami model (for LOS conditions), the coefficient of the  $\log(f)$  term is assumed to be 20.

### III. RESULTS AND DISCUSSION

The parameters of the frequency-specific one-slope models, i.e., the path loss  $PL(d_0)$  at  $d_0 = 1$  m, the path-loss expo-

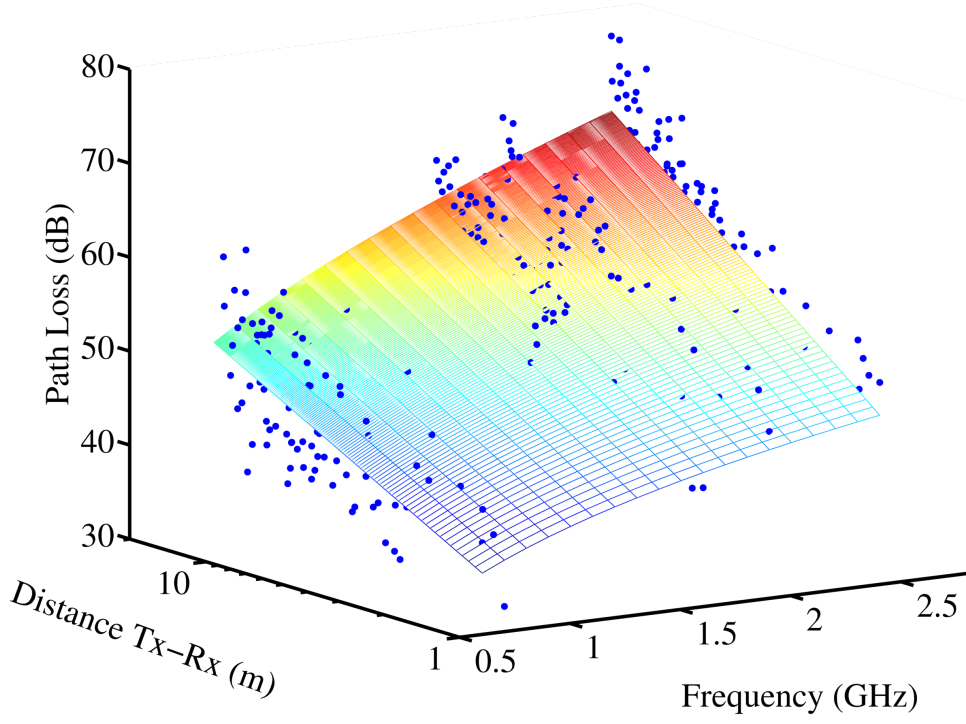


Fig. 4. Surface plot of the total path loss model, and scatter plot of the individual path loss measurements.  $R^2 = 0.77$ .

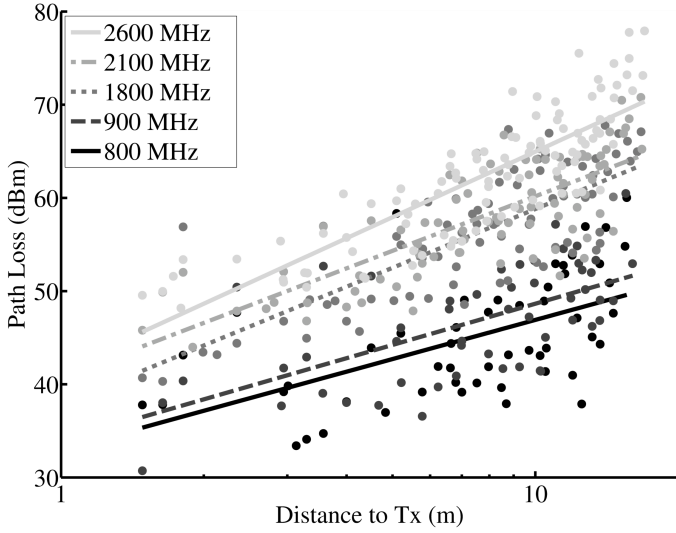


Fig. 3. Path loss scatter plots and fitted one-slope models for the different frequencies.

nent  $n$  (and their respective 95% confidence intervals), and the standard deviation  $\sigma_S$  of the variable  $\chi_S$  (see Equation (2)), are determined through a linear regression analysis of the calculated path loss samples, and are listed in Table I, along with their respective  $R^2$  (coefficient of determination) values. A visual comparison of the one-slope models and our calculations is shown in Figure 3.

$PL(d_0)$ , the path-loss value at  $d_0 = 1$  m, increases monotonously with the frequency, from approximately 33 dB

at 800 MHz to close to 42 dB at 2600 MHz. The path loss exponent,  $n$ , in general, also increases monotonously with the frequency. At the lower frequencies of 800 MHz and 900 MHz, the smaller  $n$ , respectively 1.39 and 1.47, are an indication of the waveguide effect of the elongated metal cage that is the car. At higher frequencies, the increasing influence of the seats on the propagation results in larger path loss exponents, e.g., 2.33 at 2600 MHz.

Compared to [3], we obtain a larger path loss exponent at 2100 MHz (1.9 compared to 1.2-1.6). However, we also find that the path loss is less than 70 dB throughout the car at this frequency. Furthermore, the maximum path loss, at 2600 MHz, is below 80 dB.

The standard deviation  $\sigma_S$  of the shadow fading variable  $\chi_S$  decreases with frequency, from 5.56 dB for the 800 MHz model to 3.94 dB for the 2600 MHz model. However, this trend is probably due to the increasing number of samples, since there is no mention of a frequency dependency of  $\chi_S$  in e.g., [6].

For the same reason, the frequencies' respective one-slope models are increasingly accurate; the  $R^2$  increases from 0.32 for the 800 MHz model to 0.71 for the 2600 MHz model.

Finally, using multiple linear regression, the total data pool is fitted to the frequency-dependent path-loss model of Equations (3) and (4). The resulting parameters, and their respective 95% confidence intervals are

$$\begin{aligned} PL(d_0, f_0) &= 33.90 \text{ (32.32, 35.47) dB,} \\ n_0 &= 1.19 \text{ (0.97, 1.41),} \\ m &= 0.41 \text{ (0.34, 0.48) GHz}^{-1}, \end{aligned}$$

while the standard deviation  $\rho_S$  of the shadow fading variable  $\epsilon_S$  is 4.30 dB. The coefficient of determination,  $R^2$ , of our final model is 0.77, which is better than any of the frequency-specific one-slope models.

The surface plot of this final path-loss model and the comparison to the our path-loss calculations are shown in Figure 4.

#### IV. CONCLUSION

Considering future developments of wireless communication services onboard trains, we performed path-loss measurements at five wireless communication frequencies in a double-decker train car, and fitted them to frequency-specific one-slope models, as well as a single, frequency-dependent path-loss model, which accuracy is better than any of the individual one-slope models. The results further show a waveguide effect at lower frequencies, and path-loss exponents close to 2 (free space) at higher frequencies, while the total path loss is less than 80 dB throughout the train car, indicating that coverage in a single car using miniature, WiFi-like base stations (e.g., femtocells) can be easily and efficiently obtained.

#### ACKNOWLEDGMENT

This work has been carried out with the financial support of the Interdisciplinary institute for BroadBand Technology (IBBT) project 'Railway Applications Integration and Long-term networkS (RAILS)'. W. Joseph and E. Tanghe are Post-Doctoral Fellows of the FWO-V (Research Foundation-Flanders).

#### REFERENCES

- [1] S. Knorzer, M. A. Baldauf, T. Fugen, and W. Wiesbeck, *Channel Analysis for an OFDM-MISO Train Communications System Using Different Antennas*. VTC 2007-Fall, pp. 809-813, Oct. 2007.
- [2] L. Verstrepen, W. Joseph, E. Tanghe, D. Pareit, D. Naudts, J. Keymeulen, P. De Cleyn, C. Blondia, L. Martens, and I. Moerman, *Models for wireless data communications in indoor train environment*. Wireless Personal Communications. Sep. 2011.
- [3] N. Kita, T. Ito, M. Yamada, Y. Sagawa, M. Ogasawara, and M. Nakatsugawa, *Experimental study of path loss characteristics in high-speed train cars*. In Proceedings of the 2009 IEEE Antennas and Propagation Society International Symposium. Charleston, SC, USA, 2009.
- [4] R. A. Valenzuela, O. Landron, and D. L. Jacobs, *Estimating local mean signal strength of indoor multipath propagation*. IEEE Trans. Veh. Technol., vol. 46, no. 1, pp. 203-212, Feb. 1997.
- [5] S. R. Saunders, *Antennas and Propagation for Wireless Communication Systems*. Wiley and Sons, 1999.
- [6] E. Tanghe, W. Joseph, L. Verloock, L. Martens, H. Capoen, K. Herwegen, and W. Vantomme, *The industrial indoor channel: large-scale and temporal fading at 900, 2400, and 5200 MHz*. IEEE Trans. Wireless Commun. vol. 7, no. 7, pp. 2740-2751, July 2008.